CrossMark

Oscillating Adriatic temperature and salinity regimes mapped using the Self-Organizing Maps method

Frano Matić[a], Z Žarko Kovač[a,*], Ivica Vilibić[a], Hrvoje Mihanović[a], Mira Morović[a], Branka Grbec[a], Nenad Leder[b], Tomislav Džoić[a]

[a] *Institute of Oceanography and Fisheries, Šetalište I. Meštrovića 63, 21000 Split, Croatia*
[b] *Hydrographic Institute of the Republic of Croatia, Zrinsko-Frankopanska 161, 21000 Split, Croatia*

ARTICLE INFO

ABSTRACT

This paper aims to document salinity and temperature regimes in the middle and south Adriatic Sea by applying the Self-Organizing Maps (SOM) method to the available long-term temperature and salinity series. The data were collected on a seasonal basis between 1963 and 2011 in two dense water collecting depressions, Jabuka Pit and Southern Adriatic Pit, and over the Palagruža Sill. Seasonality was removed prior to the analyses. Salinity regimes have been found to oscillate rapidly between low-salinity and high-salinity SOM solutions, ascribed to the advection of Western and Eastern Mediterranean waters, respectively. Transient salinity regimes normally lasted less than a season, while temperature transient regimes lasted longer. Salinity regimes prolonged their duration after the major basin-wide event, the Eastern Mediterranean Transient, in the early 1990s. A qualitative relationship between high-salinity regimes and dense water formation and dynamics has been documented. The SOM-based analyses have a large capacity for classifying the oscillating ocean regimes in a basin, which, in the case of the Adriatic Sea, beside climate forcing, is an important driver of biogeochemical changes that impacts trophic relations, appearance and abundance of alien organisms, and fisheries, etc.

1. Introduction

The mapping of characteristic patterns, regimes and shifts, currently used in the long-term observational and modelling series of ocean climate studies, is based on a variety of algorithms (Thomson and Emery, 2014). The most common approaches include principal component analysis (PCA, Preisendorfer and Mobley, 1988), regime shift analyses (Rodionov, 2004) and most recently, neural network algorithms, which are primarily used for pattern recognition (Jain et al., 2000). The Self-Organizing Maps (SOM) method, or Kohonen maps (Kohonen, 1982, 2001), is particularly useful in geosciences, with applications ranging from data analysis and classification (Tambouratzis and Tambouratzis, 2008) to mapping of remotely sensed data (Richardson et al., 2003; Liu et al., 2007) and climate simulations/projections (Yip and Yau, 2012). The method has widespread use in other fields of science, with a rapidly increasing number of publications (Pöllä et al., 2009).

In the Adriatic Sea, the SOM method has been used extensively for mapping different oceanographic parameters, with applications ranging from high-frequency radar data (Mihanović et al., 2011) through long-term oceanographic parameters (Vilibić et al., 2011; Mihanović

et al., 2015), underwater noise distributions (Rako et al., 2013), remotely sensed chlorophyll (Kovač et al., 2014) and biogeochemical data (Solidoro et al., 2009). SOM-based mapping of long-term oscillations of thermohaline properties, recently explained by internal dynamics (Gačić et al., 2010), have been exposed to decadal time scale oscillations, have shown dominating changes in oceanographic properties and have been known to occur for a half-century in the Adriatic (Buljan, 1953). The so-called Adriatic-Ionian Bimodal Oscillating System (BiOS), driven by the Adriatic dense water outflow towards the Ionian Sea and advection of either low-salinity Western Mediterranean waters (Modified Atlantic Water, MAW) or high-salinity Eastern Mediterranean waters (Levantine Intermediate Water, LIW), has been found useful in identifying a number of oscillatory patterns in the Adriatic, including biogeochemical properties (Civitarese et al., 2010), advection of foreign species (Batistić et al., 2014), and oscillations in fish stock and fish biology (Grbec et al., 2015; Vilibić et al., 2016).

Dense water formation (DWF), the BiOS generator, occurs during pronounced wintertime outbreaks (Mihanović et al., 2013) of cold and dry bora wind (Grisogono and Belušić, 2009) in two distinct Adriatic regions: a wide northern Adriatic shelf (Vested et al., 1998) and a deep

---

South Adriatic Pit (Gačić et al., 2002). Aside from effects it has on the BiOS regimes, DWF is responsible for ventilation of deep Adriatic waters (Gačić et al., 2002) and for driving the thermohaline circulation of the Adriatic (Vilibić et al., 2013). Two of the four major Adriatic water masses, North Adriatic Dense Water (NAdDW) and Adriatic Deep Water (AdDW), are generated via DWF, flowing out of the basin and feeding deep layers of the Eastern Mediterranean (Robinson et al., 1992). Interplay amongst all of the above processes drives seasonal, interannual, and decadal oscillations of thermohaline and biogeochemical properties in the Adriatic. Classification and mapping of these oscillations has been recognized as an important topic in Adriatic research (Mihanović et al., 2015). It seems that decadal oscillations in the Adriatic are correlated with sea surface height in the northern Ionian gyre (Gačić et al., 2010), opening possibilities for a short-term qualitative forecast of Adriatic properties, including regime shifts recently documented in the Adriatic (Grbec et al., 2009; Matić et al., 2011).

This paper, using SOM methodology, maps temperature and salinity changes in the Adriatic Sea in the last half century and classifies Adriatic temperature and salinity regimes. Section 2 describes the data used in the study and the SOM method. Section 3 presents the mapping of data, the analysis of salinity and temperature regimes and their stability and interconnectivity. Finally, conclusions are provided in Section 4.

2. Data and methods

2.1. The data

Measurements were performed between 1963 and 2011 on six long-term oceanographic stations in the central and southern Adriatic: P1 through P6 (Fig. 1). Sampling was performed seasonally, typically in March, June, September and December. During the period between 1963–1987, reversing thermometers and Nansen bottles (classic oceanographic measurements) were used to measure ocean temperature and salinity, the latter being determined through titration. The accuracy was ± 0.02 ℃ and ± 0.02 for temperature and salinity, respectively. Since 1987, measurements were also performed using the SeaBird 911 CTD probe, continuing after 1997 with the SeaBird 911, SeaBird 25 and Idronaut 316 CTD probes solely. The accuracy of the data obtained by these probes was ± 0.001 ℃ and ± 0.0001 S/m for temperature and conductivity, respectively. The instruments were calibrated on a regular basis. Details about the methodology and quality control of the data are well documented by Buljan and Zore-Armanda (1966, 1979), Zore-Armanda et al. (1991), Grbec and Morović (1997), Matić et al. (2011) and Vilibić et al. (2011, 2013). The data are available in publications by Buljan and Zore-Armanda (1966, 1979) and Zore-Armanda et al. (1991), while recent data are stored in the data bases of the Institute of Oceanography and Fisheries - Split and the Hydrographic Institute of the Republic of Croatia – Split.

Measurements were conducted at standard oceanographic depths (0, 10, 20, 30, 50, 75, 100, 150, 200, 300, 400, 500, 600, 800, 1000, 1200 m and bottom); a single cruise encompassed 57 temperature and 57 salinity measurements at maximum, spanning all stations and depths. Each data series was normalized by using respective seasonal mean and standard deviation (for full length period), which is a prerequisite for equal treatment of different parameters by the SOM analysis (Mihanović et al., 2011).

The cruises did not necessarily include all stations during a certain campaign. Temperature and salinity were measured at the stations: P1 on 56% of cruises, 95% at P2, 77% at P3, 67% at P4, 66% at P5 and 40% at P6. The most frequent sampling period was from 1966 to 1979, which contained no data gaps, followed by quasi-randomly distributed
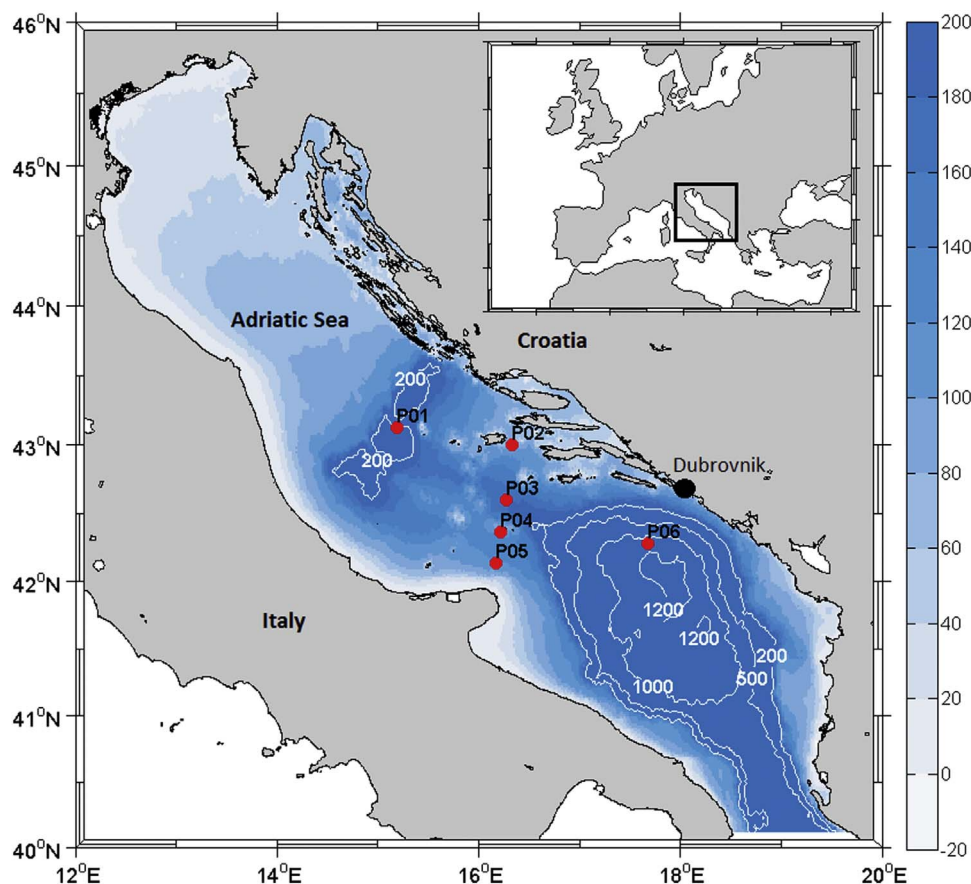

Fig. 1. Map of the Adriatic Sea with position of the climatological oceanographic stations P1 to P6.

gaps in the series.

2.2. SOM method

The SOM method, known also as Kohonen maps (Kohonen, 1982, 2001; Kriesel, 2007) represents an unsupervised clustering method based on a neural network model. The data introduced to SOM are nonlinearly projected onto a regular grid composed of neurons. Adjacent units on the grid are called neighbours, while their inter-connection is parameterized by a neighbourhood function. Input data vectors are presented to SOM and the activation of each neuron is calculated using an activation function, commonly being the Euclidian distance between the weight vector of the neuron and the input vector. The weight vector of the neuron showing the highest activation (i.e., smallest Euclidian distance) is selected as the "winner". In each successive step, the node with the highest activation is selected, and its weight vector, along with the weight vectors of the neighbourhood neurons, alters to match the data as closely as possible. The winning neuron stands as the best representation of the input data by the SOM network at an iterative stage of the training process. The network attempts to take the shape of the input data, until the best possible fit of the SOM network to the data is reached. At the final stage, the method results with a set of neurons (patterns of data), effectively reducing the complexity of the data set to a smaller number of patterns. When data are compared to the trained network, the winning neuron is declared as the best-matching unit (BMU) for a given data vector. More technical details about the method and its application to oceanographic problems is documented by Liu et al. (2006, 2007), Liu et al. (2011) and Mihanović et al. (2011).

A noticeable advantage of the SOM method over other pattern-extracting methods, such as PCA, is that the method has an ability to work on data that contains gaps. That is particularly useful for mapping patterns that come from different hydrographic surveys (e.g., Vilibić et al., 2011), where not all prescribed stations nor depths are sampled during a specific cruise. As our hydrographic series has a substantial portion of data gaps, we presumed that the SOM method is more reliable for detecting oscillating regimes than other pattern-creating methods (Mihanović et al., 2011). Additionally, the SOM method extracts non orthogonal (asymmetric) patterns, while by default, all modes of PCA are mutually orthogonal (Liu and Weisberg, 2007). SOM asymmetric patterns can describe similar oceanographic processes that are not observed in PCA modes (Mihanović et al., 2015).

In this paper, the following parameters have been selected in the SOM analysis: the rectangular neural lattice of "sheet" shape, the linear SOM initialization, the "ep" neighbourhood function, and the batch training algorithm. The number of iterations was set to "long". This selection was chosen following recommendations from previous SOM studies (e.g., Liu et al., 2006; Vilibić et al., 2011). The SOM array was set to 3×3 (9 patterns), which represents a good compromise between data details and visualization potential.

3. Results and discussion

Normalized temperature anomaly SOM patterns are displayed in Fig. 2, with its salinity counterparts shown in Fig. 3. We defined the anomaly index as an average anomaly over each pattern, ranging from −0.49 to 0.47. The index range was divided into three equally distant parts and was associated with a positive, neutral or negative pattern anomaly: BMU1-2-3, BMU4-5-6 and BMU7-8-9 are therefore classi-fied as the T⁻, T° and T⁺ regimes, respectively, while BMU1-4-7, BMU2-5 and BMU3-6-8-9 are associated to the S⁻, S° and S⁺ regimes, respectively.

The patterns are spread out over neurons, with BMU1 allocated to the lowest salinity and temperature, and at the opposite end, with BMU9 allocated to the highest temperature and salinity. It is interest-ing to note that temperature and salinity anomalies are organized in

different ways: salinity BMU states are arranged vertically over nodes, with BMU1-4-7, BMU2-5 and BMU3-6-8-9 associated with low, neutral and high salinities, respectively, while temperature BMU states are arranged horizontally, with BMU1-2-3, BMU4-5-6 and BMU7-8-9 representing low, neutral and high temperatures.

The two most distant patterns (BMU1 and 9) reveal a layered distribution of the temperature anomaly along the vertical, keeping the most pronounced anomaly in intermediate layers. This indicates a strong horizontal advection occurring over the entire middle and southern Adriatic, as a thermohaline gradient is normally present along the southern and middle Adriatic (Artegiani et al., 1997). By contrast, BMU2-3-4-5-6 exhibits a quasi-homogeneous temperature anomaly distribution over Palagruža Sill, which indicates a low horizontal advection or an existence of pronounced vertical processes and mixing.

Spatial salinity anomaly BMU fields appear more homogenous, with no significant differences between western and eastern parts of the Sill. Yet, the very bottom of the Jabuka Pit station is characterized by a temperature anomaly opposing from the intermediate layer for BMU 1-2-3-8-9. Notably, the negative temperature anomaly at the bottom of the Jabuka Pit for BMU8-9 (28% of all SOM solutions) is related to the largest positive anomaly in temperature and salinity in the intermedi-ate layer.

Comparing these regimes to Adriatic water masses (Zore-Armanda, 1963), S⁺ patterns may be associated to the advection of saline LIW from the Eastern Mediterranean, while S⁻ patterns are representative of waters coming from the Western Mediterranean. In other words, S⁺ patterns are probably associated with a cyclonic BiOS regime, opposite to S⁻ patterns, which are presumably a product of anticyclonic circulation in the Northern Ionian Sea (Gačić et al., 2010). S° patterns are transitional, mostly occurring between S⁺ and S⁻ regimes. Temperature patterns associated with a particular salinity regime span a variety of ranges, indicating that either (i) LIW or MAW may vary in temperature, which is determined by the rate of heat loss in the generation area (e.g., in Rhodes Gyre, Robinson et al., 1992, or Western Mediterranean), or (ii) LIW/MAW temperature may be modified in the Adriatic Sea during cooling events, as S⁺/S⁻ regime may be adjoined with warm winters and low heat losses or with cold winters and strong heat losses, causing a substantial decrease in temperature of the originally advected LIW/MAW (Mantziafou and Lascaratos, 2008; Oddo and Guarnieri, 2011).

It is interesting to note that the frequency of the S° regime (Fig. 3) is very low (6%, BMU2-5), indicating that the salinity regimes in the Adriatic tend to exist in high-low regimes and that transitions from S⁺ to S⁻, and vice versa, occur rapidly. By contrast, temperature transitions are occurring more gradually, as the T° regime (Fig. 2) accounts for 21% of all SOM patterns (BMU4-5-6).

However, BMU8 and BMU9, associated with the S⁺ regime (Fig. 3), are linked with the highest negative temperature anomalies (Fig. 2) at the bottom of both Adriatic depressions, the Jabuka Pit below 175 m and the Southern Adriatic Pit below 800 m. Both depressions are known to collect NAdDW at their deepest depths (Vilibić and Šantić, 2008; Bensi et al., 2013; Mihanović et al., 2013), below the depths of adjacent sills, the Palagruža Sill and the Otranto Strait, so a direct link exists between the strong inflow of LIW to the Adriatic and the strong DWF in the northern Adriatic. It is known that the strong DWF in the Adriatic and the outflow of dense waters in the form of bottom density currents drive the Adriatic thermohaline circulation and lagged LIW inflow all the way to the northern Adriatic (Orlić et al., 2007). Distributions of temperature and salinity anomalies over the S⁺ regime support this observation, as the stronger DWF (lower temperatures at depressions) are associated with higher LIW transport to the Adriatic (higher salinities). These patterns (Fig. 4) are found in years when NAdDW was documented at the Jabuka Pit, 1971, 1981, 1982, 1987, 1989, 1999, 2000, but also in years with strong LIW inflow, 1986, 1969, 1971, 1980, 1987–1989 (Vilibić et al., 2011; Vilibić and Supić,
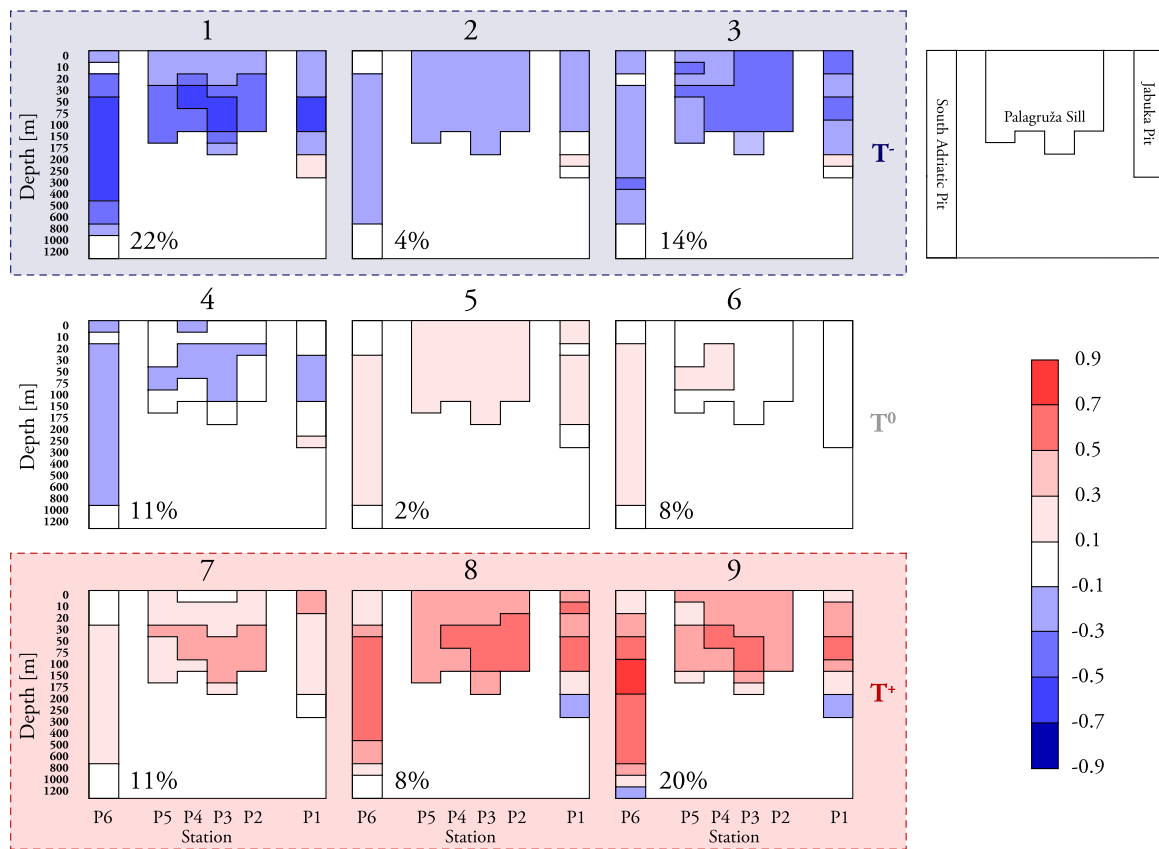
Fig. 2. 2D representation of spatial distribution of sea temperature anomaly for BMUs classified to anomaly intensity into three classes (T⁻, Tº and T⁺). Relative appearance of each neuron is written on left bottom corner of each picture.
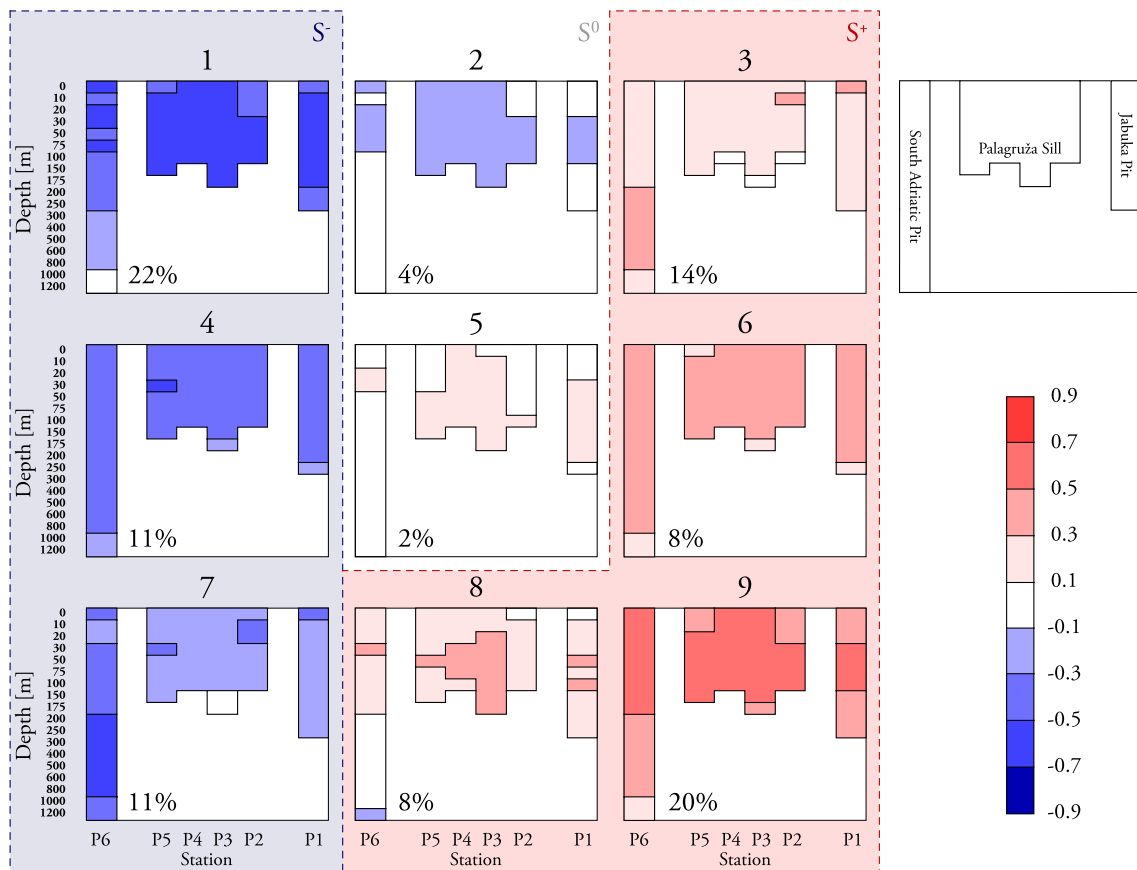

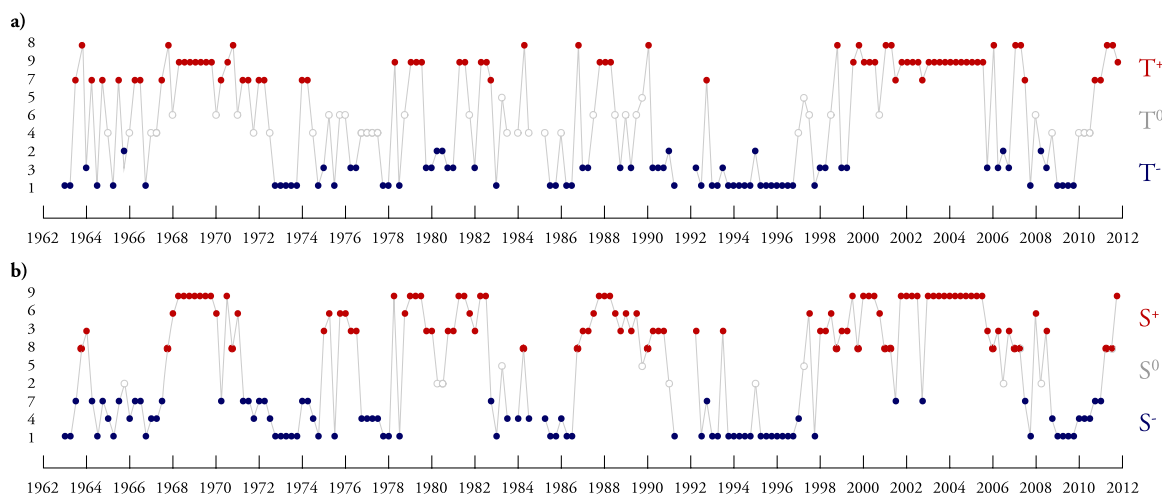Fig. 3. As in Fig. 2, but for salinity anomaly regimes (S⁻, Sº, S⁺).

Fig. 4. BMU time series sorted and coloured according to (a) temperature and (b) salinity regimes.

2005). NAdDW formed in 1984, 1991 and 2006 was not detected in our analysis, resulting from a measurement gap at the P1 station.

Unlike BMU8-9, the BMU1-2-3 associated with the T⁻ regime had slight positive temperature anomalies at the bottom of the Jabuka Pit. BMU1-2 are also characterized by low salinity values, which are a footprint of the anticyclonic BiOS phase, advecting low salinity waters up to the northern Adriatic. These waters normally prevent DWF and the generation of dense waters that are capable of sinking to the bottom of the pits; thus, warmer than usual and older water masses are normally found in the Jabuka Pit that are associated with these patterns.

Although there are some along-basin differences and variations in the vertical, both T (Fig. 2) and S (Fig. 3) anomalies are quasi-homogeneously distributed over all stations and areas (SAP, Palagruža Sill and Jabuka Pit) for a certain BMU pattern. Therefore, LIW or MAW intrusions to the Adriatic occur quasi-simultaneously at the seasonal timescale, where transport is not stopped by the shallow Palagruža Sill (maximum depths reaching 170 m), a barrier which deflects most of the incoming Eastern Adriatic Current towards a permanent cyclonic gyre within the deep SAP (Poulain, 2001). In other words, the overflow of intermediate waters from the SAP to the Jabuka Pit and the longitudinal exchange of water masses over the Palagruža Sill always lasts less than 3 months. This finding is in agreement with numerical modelling studies, which show a permanent EAC inflow over central parts of the Palagruža Sill, although being modified in time by wind and freshwater buoyancy forcing (Martin et al., 2009).

Temporal changes of BMUs, plotted for temperature (upper plot) and salinity (lower plot) regimes, are displayed in Fig. 4. Both graphs indicate a strong variability on a decadal scale, which is much more pronounced in salinity regimes. Salinity regimes, referred to as "Adriatic ingressions" (Buljan, 1953), have been known to occur for a long time and are well documented in Adriatic water mass studies (Zore-Armanda, 1963; Buljan and Zore-Armanda, 1976; Zore-Armanda et al., 1991) and have been recently associated to internal (Gačić et al., 2010; Mihanović et al., 2015) or wind-driven (Pinardi et al., 2013; Shabrang et al., 2016) decadal variations in the northern Ionian Sea. However, it seems that these regime shifts in the Adriatic Sea occur quite rapidly, as either no transitional pattern or just one (S⁰) was found to occur during these transitions. Moreover, quite rapid transitions between extreme BMU patterns, BMU1-4 and BMU6-9, in less than a year are sometimes found, e.g., in 1967, 1974, 1978, 1982/1983, indicating that the replenishment of the middle and south Adriatic waters may occur rapidly, in less than a year. These rapid changes may also be observed in a series of averaged anomalies from the SOM patterns of temperature and salinity data in the 50–500 m deep layer (Fig. 5), in which LIW/MAW advection is normally

occurring. This appears to contrast the value provided by Vilibić and Orlić (2002), which estimated a decay time of 26 months for replenishment of the Adriatic waters. The ventilation of the Adriatic is probably variable in time and can occur more rapidly during the BiOS regime changes and more slowly during a prolonged BiOS regime. This hypothesis is worth future research, given that ventilation of the Adriatic is important for the biogeochemistry and ecosystems of the deep Adriatic.

Once plotted, the BMU series for temperature regimes (Fig. 4a) display transitions that occur less rapidly, confirming that temperature is not the primary variable describing decadal variations in the Adriatic. However, the similarities between the S and T regimes is more noticeable after the early 1990s rather than prior, probably due to the major event, the Eastern Mediterranean Transient, that affected thermohaline properties of the entire Eastern Mediterranean, (EMT, Klein et al., 1999). Aside from its major effects on deep Eastern Mediterranean waters, the EMT strengthened and increased the period of decadal oscillations in the Adriatic and thus increased the role of the advected waters, both directly and as a preconditioning to the DWF, in shaping thermohaline properties of the Adriatic.

To support the above hypothesis, a sequential algorithm for testing climate regime shifts was applied on the normalized T and S BMU time series that averaged between 50 m and 500 m and is presented in Fig. 5, with the following algorithm parameters: significance level p=0.01, cutoff length l =5 years, and Huber's weight parameter H =1 (Rodionov, 2004). In the period between 1963 and 2011, there were three climate regimes in the temperature time series: the first between 1967 and 1972, the second between 1990 and 1998 and third between 1999 and 2005. In the same period, there were eight regimes in the salinity time series: 1963–1967, 1968–1971, 1972–1978, 1978–1982, 1983–1986, 1987–1990, 1991–1997 and 1998–2007. Apparently, the duration of temperature and salinity regimes increased in the last two decades. Future research should quantify these processes as there is presumably a regime shift in the Adriatic being driven from a variety of ocean variables, from thermohaline properties, nutrients, primary production, fisheries, etc. (Dulčić et al., 2007; Grbec et al., 2008, 2009, 2015; Vilibić et al., 2012, 2016).

Salinity regimes (S⁻, S⁰, S⁺), as observed by BMU patterns, are somewhat less stable than climate regimes, as computed by the above sequential algorithm, as an anomalous departure from a salinity regime may last for a season or a few seasons, which is uncounted for when computing a climate shift following Rodionov's (2004) methodology. To augment this analysis, connectivity diagrams (Fig. 6) were formed from the transitional probabilities of an individual BMU by counting the number of BMU transitions from a given state to another one, divided by the total number of state transitions made by that BMU.
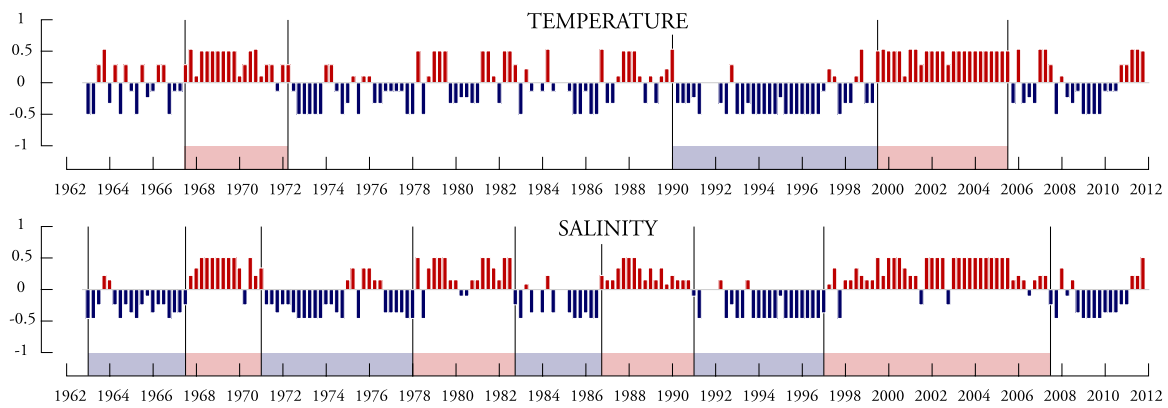
Fig. 5. Temporal evolution of averaged anomalies from SOM 3×3 patterns of sea temperature and salinity of Adriatic Sea intermediate layer (50–500m).

Fig. 6 shows the stability of S$^-$ and S$^+$ regimes, which equalled 79% and 76%, respectively. In other words, the average duration of a regime before switching to two other regimes equals 2–3 years. However, the stability of S$^-$ and S$^+$ regimes increases to 88% and 91% (average regime duration of approximately 5–8 years), respectively, if departures to other regimes, which last less than 6 months, are excluded (e.g., as occurring in 1963, 1984, 1993, etc., Fig. 4b).

One of the most frequent SOM patterns (20%), BMU9, is also the most stable pattern, which preserves its stability in 71% of its connections (i.e., it is followed by itself), or it is followed by BMU6 (10%) or by other salinity regimes (19%). On the side of the SOM distributions, BMU1 is the most frequent (22%) and most stable S$^-$ regime pattern (52%), from which the other salinity regimes (S^o, S$^+$) are followed in 15% of all connections. It is interesting to note that there are no connections between BMU8 and BMU6-9; BMU8 is mostly a transitional pattern to other salinity regimes (80%).

4. Conclusions

This paper attempts to classify Adriatic thermohaline variations by applying a neural network algorithm, SOM, to a half-century time series of temperature and salinity measured at the middle Adriatic constriction, Palagruža Sill, and two adjacent depressions, Jabuka Pit and Southern Adriatic Pit. The latter has been known to serve as a collector of dense waters. In addition to other Adriatic studies of long-term thermohaline changes (Grbec et al., 2009, 2015; Matić et al., 2011; Vilibić et al., 2011, 2012, 2013; Mihanović et al., 2015), the following conclusions should be considered:

(i) Two basic patterns may be found in the middle and south Adriatic, the first identifies pronounced vertical anomaly gradients, indicat-

ing a strong horizontal advection, and the second, with basin-scale uniformity in anomalies, indicates either low horizontal processes or strong vertical mixing (e.g., coming from deep convection),

(ii) Transitions between high and low salinity regimes occur rapidly, in less than half a year, acting over an order of magnitude that is shorter in timescale compared with the major driving mechanism (BiOS),

(iii) The duration of temperature and salinity regimes has been prolonged since the early 1990s, matching the period of the Eastern Mediterranean Transient influence to Adriatic oceanographic properties (Vilibić et al., 2012),

(iv) The regimes of temperature and salinity in the Adriatic Sea significantly differ from each other. Salinity regimes respond to long-term fluctuations of the Mediterranean flow into the Adriatic Sea, driven predominantly by the BiOS. Temperature regimes have shorter periodicity, being presumably affected by processes restricted to the Adriatic besides the advective influence from the Mediterranean, such as extensive heat losses occurring during wintertime cooling events (e.g., Oddo and Guarnieri, 2011; Mihanović et al., 2013) that substantially influence the Adriatic temperature conditions.

All these conclusions point to a robustness of the SOM method as an assessment of oceanographic patterns derived from long-term measurements. Unlike PCA method, the SOM method is tolerant to missing values and is capable to detect asymmetric patterns not found in individual PCA modes. Specifically, Liu et al. (2006) showed that the SOM method was successful in extracting all complex patterns from multiple artificial data sets, while the PCA method failed to do that. On the other hand, PCA preserves variance and the original data may be identically reconstructed, while SOM is not a straightforward method
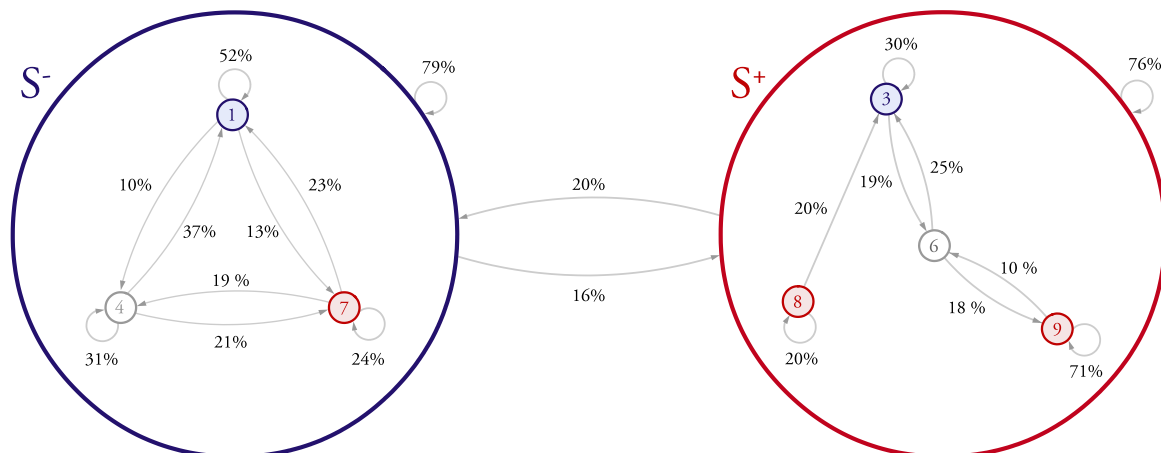

Fig. 6. Connectivity diagrams for S$^-$ and S$^+$ salinity regimes, with percentages of connections between different BMU.

for reconstructing the data since it preserves data topology, not variance. Although the series analysed in this study contained large gaps, with less than half of the data available at certain stations (station P6), the patterns that were observed deepen the existing knowledge of the Adriatic thermohaline circulation, and no conflicting results were documented. The method was capable of distinguishing rapid changes in Adriatic characteristic patterns, nominating its application to other ocean basins where long-term hydrographic measurements are available, or to the mapping of different sets of parameters, e.g., biogeochemical (Dufois et al., 2014) and fisheries parameters (Conti et al., 2012). The method also performed well in determining bimodal oscillatory patterns, already known to occur in the Adriatic (Gačić et al., 2010) showing that SOM has a large application potential in mapping different ocean oscillatory processes that are normally an important ingredient in a large number of oceans and coastal basins (e.g., Zeng et al., 2015).

In addition to long-term in situ observations, regional climate model runs (e.g., for the Mediterranean, Sevault et al., 2014) spanning several decades are also suitable for mapping oscillatory patterns in the Adriatic-Ionian basin and should take priority in future research. It is reasonable to hypothesize that occurrences of extreme events are expected to be more frequent and stronger in a warming climate, presumably affecting the periodicity of oscillating regimes (Nissen et al., 2014). Knowledge about Adriatic oscillatory patterns induced by the oscillatory BiOS regime or by transient massive events such as the EMT is of utmost importance for Adriatic thermohaline and biogeochemistry patterns, trophic structure and fisheries, and forecasting via climate scenario simulations and should be a tool for their assessment in the future.

Acknowledgements

References

Artegiani, A., Bregant, D., Paschini, E., Pinardi, N., Raicich, F., Russo, A., 1997. The Adriatic Sea general circulation. Part I: air–sea interactions and water mass structure. J. Phys. Oceanogr. 27, 1492–1514. http://dx.doi.org/10.1175/1520-0485(1997)027 < 1492:TASGCP > 2.0.CO;2.

Batistić, M., Garić, R., Molinero, J.C., 2014. Interannual variations in Adriatic Sea zooplankton mirror shifts in circulation regimes in the Ionian Sea. Clim. Res. 61, 231–240. http://dx.doi.org/10.3354/cr01248.

Bensi, M., Cardin, V., Rubino, A., Notarstefano, G., Poulain, P.-M., 2013. Effects of winter convection on the deep layer of the Southern Adriatic Sea in 2012. J. Geophys. Res. 118, 6064–6075. http://dx.doi.org/10.1002/2013JC009432.

Buljan, M., 1953. Fluctuation of salinity in the Adriatic. Izvještaj Republičke Ribarstveno-biološke ekspedicije "Hvar" 1948–1949. Acta Adriat. 2 (2), 1–64.

Buljan, M., Zore-Armanda, M., 1966. Hydrographic data on the Adriatic Sea collected in the period from 1952 through 1964. Acta Adriat. 12, 1–438.

Buljan, M., Zore-Armanda, M., 1976. Oceanographic properties of the Adriatic Sea. Oceanogr. Mar. Biol. Rev. 14, 11–98.

Buljan, M., Zore-Armanda, M., 1979. Hydrographic properties of the Adriatic Sea in the period from 1965 through 1970. Acta Adriat. 20, 1–368.

Civitarese, G., Gačić, M., Lipizer, M., Borzelli, G.L.E., 2010. On the impact of the Bimodal Oscillating System (BiOS) on the biogeochemistry and biology of the Adriatic and Ionian Seas (Eastern Mediterranean)Biogeosciences 7, 3987–3997. http://dx.doi.org/10.5194/bg-7-3987-2010.

Conti, L., Grenouillet, G., Lek, S., Scardi, M., 2012. Long-term changes and recurrent patterns in fisheries landings from large marine ecosystems (1950–2004). Fish. Res. 119–120, 1–12. http://dx.doi.org/10.1016/j.fishres.2011.12.002.

Dufois, F., Hardman-Mountford, N.J., Greenwood, J., Richardson, A.J., Feng, M., Herbette, S., Matear, R., 2014. Impact of eddies on surface chlorophyll in the South Indian Ocean. J. Geophys. Res. 119, 8061–8077. http://dx.doi.org/10.1002/2014JC010164.

Dulčić, J., Beg Paklar, G., Grbec, B., Morović, M., Matić, F., Lipej, L., 2007. On the occurrence of ocean sunfish Mola mola and slender sunfish Ranzania laevis in the eastern Adriatic. J. Mar. Biol. Assoc. U. Kingd. 87, 789–796. http://dx.doi.org/10.1017/S0025315407053842.

Gačić, M., Civitarese, G., Miserocchi, S., Cardin, V., Crise, A., Mauri, E., 2002. The open-ocean convection in the Southern Adriatic: a controlling mechanism of the spring phytoplankton bloom. Cont. Shelf Res. 22, 1897–1908. http://dx.doi.org/10.1016/S0278-4343(02)00050-X.

Gačić, M., Borzelli, G.L.E., Civitarese, G., Cardin, V., Yari, S., 2010. Can internal processes sustain reversals of the ocean upper circulation? The Ionian Sea example. Geophys. Res. Lett. 37, L09608. http://dx.doi.org/10.1029/2010GL043216.

Grbec, B., Morović, M., 1997. Seasonal thermohaline fluctuations in the middle Adriatic sea. Il Nuovo Cim. C 20 (4), 561–576.

Grbec, B., Morović, M., Dulčić, J., Marasović, I., Ninčević, Ž., 2008. Impact of the climatic change on the Adriatic Sea ecosystem. Fresenius Environ. Bull. 17, 1615–1620.

Grbec, B., Morović, M., Beg Paklar, G., Kušpilić, G., Matijević, S., Matić, F., Gladan, Ž.N., 2009. The relationship between the atmospheric variability and productivity in the Adriatic Sea area. J. Mar. Biol. Assoc. U. Kingd. 89, 1549–1558.

Grbec, B., Morović, M., Matić, F., Ninčević, Ž., Marasović, I., Vidjak, O., Bojanić, N., Čikeš Keč, V., Zorica, B., Kušpilić, G., Matić-Skoko, S., 2015. Climate regime shifts and multi-decadal variability of the Adriatic Sea pelagic ecosystem. Acta Adriat. 56 (1), 47–66.

Grisogono, B., Belušić, D., 2009. A review of recent advances in understanding the meso- and microscale properties of the severe Bora wind. Tellus A 61, 1–16. http://dx.doi.org/10.1111/j.1600-0870.2008.00369.x.

Jain, A.K., Duin, R.P.W., Mao, J.C., 2000. Statistical pattern recognition: a review. IEEE Trans. Pattern Anal. Mach. Intell. 22, 4–37.

Klein, B., Roether, W., Manca, B.B., Bregant, D., Beitzel, V., Kovačević, V., Luchetta, A., 1999. The large deep water transient in the Eastern Mediterranean. Deep Sea Res. I 46, 371–414. http://dx.doi.org/10.1016/S0967-0637(98)00075-2.

Kohonen, T., 1982. Self-organized formation of topologically correct feature maps. Biol. Cybern. 69, 59–69.

Kohonen, T., 2001. Self-Organizing Maps third ed.. Springer-Verlag, New York, 501.

Kovač, Ž., Morović, M., Matić, F., 2014. Uncovering spatial and temporal patterns of Adriatic Sea colour with self-organizing maps. Int. J. Remote Sens. 35, 2105–2117. http://dx.doi.org/10.1080/01431161.2014.885667.

Kriesel, D., 2007. A Brief Introduction to Neural Networks, available at ⟨http://www.dkriesel.com⟩, (accessed 03.02.16).

Liu, Y., Weisberg, R.H., Mooers, C.N.K., 2006. Performance evaluation of the self-organizing map for feature extraction. J. Geophys. Res. 111, C05018. http://dx.doi.org/10.1029/2005JC003117.

Liu, Y., Weisberg, R.H., Shay, L.K., 2007. Current patterns on the West Florida shelf from joint Self-Organizing Map analyses of HF radar and ADCP data. J. Atmos. Ocean. Technol. 24, 702–712. http://dx.doi.org/10.1175/JTECH1999.1.

Liu, Y., Weisberg, R.H., 2011. A review of self-organizing map applications in meteorology and oceanography. In: Mwasiagi, J.I. (Ed.), Self-Organizing Maps: Applications and Novel Algorithm Design. InTech, Rijeka, Croatia, 253–272. http://dx.doi.org/10.5772/13146.

Mantziafou, A., Lascaratos, A., 2008. Deep-water formation in the Adriatic Sea: Interannual simulation for years 1979–1999. Deep Sea Res. 55 (Pt. 1), 1403–1426. http://dx.doi.org/10.1016/j.dsr.2008.06.005.

Martin, P.J., Book, J.W., Burrage, D.M., Rowley, C.D., Tudor, M., 2009. Comparison of model-simulated and observed currents in the central Adriatic during DART. J. Geophys. Res. 114, C01S05. http://dx.doi.org/10.1029/2008JC004842.

Matić, F., Grbec, B., Morović, M., 2011. Indications of climate regime shifts in the middle Adriatic Sea. Acta Adriat. 52, 235–246.

Mihanović, H., Cosoli, S., Vilibić, I., Ivanković, D., Dadić, V., Gačić, M., 2011. Surface current patterns in the northern Adriatic extracted from high frequency radar data using self-organizing map analysis. J. Geophys. Res. 116, C08033. http://dx.doi.org/10.1029/2011JC007104.

Mihanović, H., Vilibić, I., Carniel, S., Tudor, M., Russo, A., Bergamasco, A., Bubić, N., Ljubešić, Z., Viličić, D., Boldrin, A., Malačič, V., Celio, M., Comici, C., Raicich, F., 2013. Exceptional dense water formation on the Adriatic shelf in the winter of 2012. Ocean Sci. 9, 561–572. http://dx.doi.org/10.5194/os-9-561-2013.

Mihanović, H., Vilibić, I., Dunić, N., Šepić, J., 2015. Mapping of decadal middle Adriatic oceanographic variability and its relation to the BiOS regime. J. Geophys. Res. Oceans, 120. http://dx.doi.org/10.1002/2015JC010725.

Nissen, K.M., Leckebusch, G.C., Pinto, J.G., Ulbrich, U., 2014. Mediterranean cyclones and windstorms in a changing climate. Reg. Environ. Change 14, 1873–1890. http://dx.doi.org/10.1007/s10113-012-0400-8.

Oddo, P., Guarnieri, A., 2011. A study of the hydrographic conditions in the Adriatic Sea from numerical modelling and direct observations (2000–2008). Ocean Sci. 7, 549–567. http://dx.doi.org/10.5194/os-7-549-2011.

Orlić, M., Dadić, V., Grbec, B., Leder, N., Marki, A., Matić, F., Mihanović, H., Beg Paklar, G., Pasarić, Z., Vilibić, I., 2007. Wintertime buoyancy forcing, changing seawater properties and two different circulation systems produced in the Adriatic. J. Geophys. Res. 112, C03S07. http://dx.doi.org/10.1029/2005JC003271.

Pinardi, N., Zavatarelli, M., Adani, M., Coppini, G., Fratianni, C., Oddo, P., Simoncelli, S., Tonani, M., Lyubartsev, V., Dobricic, S., Bonaduce, A., 2013. Mediterranean Sea large-scale low-frequency ocean variability and water mass formation rates from 1987 to 2007: a retrospective analysis. Prog. Oceanogr. 132, 318–332. http://dx.doi.org/10.1016/j.pocean.2013.11.003.

Poulain, P.-M., 2001. Adriatic Sea surface circulation as derived from drifter data between 1990 and 1999. J. Mar. Syst. 29, 3–32. http://dx.doi.org/10.1016/S0924-7963(01)00007-0.

Pöllä, M., Honkela, T., Kohonen, T., 2009. Bibliography of Self-Organizing Map (SOM) Papers: 2002−2005 Addendum. TKK Reports in Information and Computer Science, Helsinki University of Technology, Report TKK-ICS-R23.

Preisendorfer, R.W., Mobley, C.D., 1988. Principal Component Analysis in Meteorology and Oceanography. Elsevier, Amsterdam, 425.

Rako, N., Vilibić, I., Mihanović, H., 2013. Mapping the underwater sound noise and assessing its sources by using a self-organizing maps method. J. Acoust. Soc. Am. 133, 1368−1376. http://dx.doi.org/10.1121/1.4789003.

Richardson, A.J., Risien, C., Shillington, F.A., 2003. Using self-organizing maps to identify patterns in satellite imagery. Prog. Oceanogr. 59, 223−239.

Robinson, A.R., Malanotte-Rizzoli, P., Hecht, A., Michelato, A., Roether, W., Theocharis, A., Unlüata, U., Pinardi, N., Artegiani, A., Bergamasco, A., Bishop, J., Brenner, S., Christianidis, S., Gačić, M., Georgopoulos, D., Golnaraghi, M., Hausmann, M., Junghaus, H.-G., Lascaratos, A., Latif, M.A., Leslie, W.G., Lozano, C.J., Oguz, T., O¨ szoy, E., Papageorgiou, E., Paschini, E., Rozentroub, Z., Sansone, E., Scarazzato, P., Schlitzer, R., Spezie, G.-C., Tziperman, E., Zodiatis, G., Athanassiadou, L., Gerges, M., Osman, M., 1992. General circulation of the Eastern Mediterranean. Earth Sci. Rev. 32, 285−309.

Rodionov, S.N., 2004. A sequential algorithm for testing climate regime shifts. Geophys. Res. Lett. 31, L09204. http://dx.doi.org/10.1029/2004GL019448.

Sevault, F., Somot, S., Alias, A., Dubois, C., Lebeaupin-Brossier, C., Nabat, P., Adloff, F., Déqué, M., Decharme, B., 2014. A fully coupled Mediterranean regional climate system model: design and evaluation of the ocean component for the 1980−2012 period. Tellus A 66, 23967. http://dx.doi.org/10.3402/tellusa.v66.23967.

Shabrang, L., Menna, M., Pizzi, C., Lavigne, H., Civitarese, G., Gačić, M., 2016. Long-term variability of the southern Adriatic circulation in relation to North Atlantic Oscillation. Ocean Sci. 12, 233−241. http://dx.doi.org/10.5194/os-12-233-2016.

Solidoro, C., Bastianini, M., Bandelj, V., Codermatz, R., Cossarini, G., Canu, D.M., Ravagnan, E., Salon, S., Trevisani, S., 2009. Current state, scales of variability, and trends of biogeochemical properties in the northern Adriatic Sea. J. Geophys. Res. 114, C07S91. http://dx.doi.org/10.1029/2008JC004838.

Tambouratzis, T., Tambouratzis, G., 2008. Meteorological data analysis using self-organizing maps. Int. J. Intell. Syst. 23, 735−759.

Thomson, R.E., Emery, W.J., 2014. Data Analysis Methods in Physical Oceanography, Third and revised edition. Elsevier Science, Amsterdam, London, New York. http://dx.doi.org/10.1002/int.20294.

Vested, H.J., Berg, B., Uhrenholdt, T., 1998. Dense water formation in the Northern Adriatic. J. Mar. Syst. 18, 135−160. http://dx.doi.org/10.1016/S0924-7963(98)00009-8.

Vilibić, I., Orlić, M., 2002. Adriatic water masses, their rates of formation and transport through the Otranto Strait. Deep-Sea Res. I 49, 1321−1340. http://dx.doi.org/10.1016/S0967-0637(02)00028-6.

Vilibić, I., Supić, N., 2005. Dense water generation on a shelf: the case of the Adriatic Sea. Ocean Dyn. 55, 403−415.

Vilibić, I., Šantić, D., 2008. Deep water ventilation traced by Synechococcus cyanobacteria. Ocean Dyn. 58, 119−125.

Vilibić, I., Mihanović, H., Šepić, J., Matijević, S., 2011. Using Self-Organising Maps to investigate long-term changes in deep Adriatic water patterns. Cont. Shelf Res. 31, 695−711. http://dx.doi.org/10.1016/j.csr.2011.01.007.

Vilibić, I., Matijević, S., Šepić, J., Kušpilić, G., 2012. Changes in the Adriatic oceanographic properties induced by the Eastern Mediterranean Transient. Biogeosciences 9, 2085−2097. http://dx.doi.org/10.5194/bg-9-2085-2012.

Vilibić, I., Šepić, J., Proust, N., 2013. Weakening of thermohaline circulation in the Adriatic Sea. Clim. Res. 55, 217−225. http://dx.doi.org/10.3354/cr01128.

Vilibić, I., Čikeš Keč, V., Zorica, B., Šepić, J., Matijević, S., Džoić, T., 2016. Hydrographic conditions driving sardine and anchovy populations in a land-locked sea. Mar. Mediterr. Sci.. http://dx.doi.org/10.12681/mms.1120.

Yip, Z.K., Yau, M.K., 2012. Application of artificial neural networks on North Atlantic tropical cyclogenesis potential index in climate change. J. Atmos. Ocean. Technol. 29, 1202−1220. http://dx.doi.org/10.1175/JTECH-D-11-00178.1.

Zeng, X., Li, Y., He, R., Yin, Y., 2015. Clustering of loop current patterns based on the satellite-observed sea surface height and self-organizing map. Remote Sens. Lett. 6, 11−19, (doi: 0.1080/2150704X.2014.998347).

Zore-Armanda, M., 1963. Les masses d'eau de la mer Adriatique. Acta Adriat. 10, 5−88.

Zore-Armanda, M., Bone, M., Dadić, V., Morović, M., Ratković, D., Stojanovski, L., Vukadin, I., 1991. Hydrographic properties of the Adriatic Sea in the period from 1971 through 1983. Acta Adriat. 32, 1−547.